Open Access Online Journal on Astronomy and Astrophysics
Acta Astrophysica Taurica
www.astrophysicataurica.org

Acta Astrophys. Tau. 6(2), 7–13 (2025)

On the concept of spectral radiometry on RATAN-600

V.M. Bogod, M.K. Lebedev, N.E. Ovchinnikova, A.M. Ripak, A.A. Storozhenko, E.A. Kurochkin

Special Astrophysical Observatory, Nizhnij Arkhyz 369167, Zelenchukskiy region, Karachai-Cherkessian Republic, Russia
e-mail: vbog_spb@mail.ru

Received 1 October 2023

ABSTRACT

We present the results of new observations of radio emission from the solar corona in the range 1–3 GHz using RATAN-600. The difficulties of observations in this range are caused by a large amount of industrial interference (mobile communications, satellite navigation, microwave ovens, aircraft radars, etc.). Problems related to the conversion of magnetic energy into the energy of flares, heating of the corona, the role of narrow-band phenomena, and quasiperiodic pulsations in the solar corona still remain relevant. A change in the concept of the receiving spectral equipment for the RATAN-600 radio telescope has become urgent. SAO RAS is currently working on the creation of a series of next-generation spectral complexes to cover the entire operating range of RATAN-600. In this paper, we present the results of the first series of observations made with the panoramic spectral radiometric complex in the range of 1–3 GHz for studying low-contrast coronal structures. It has become feasible to implement observation modes for various objects: from powerful flaring radio sources to faint structures down to the radio granulation level. High-speed instruments for radio signal reception and information processing have been developed and introduced in order to separate useful signals from interference in real-time mode. These parameters, combined with a large effective area and wide frequency coverage of RATAN-600, allowed for observations of weak coronal structures in the frequency range of 1–3 GHz. We discuss the results of the first series of observations of weak coronal structures and their interpretation in terms of their impact on thermal processes in the corona.

Key words: Sun, radio telescope, observations, spectrum, principal component analysis

1 Introduction

The problem of studying radio emission from the solar corona lies in the need for exploring low-contrast structures against the background of a powerful signal from the quiet Sun to elucidate the nature of coronal heating. Ground-based and space observations indicate the localization of flaring processes at the tops of coronal loops that reflect the structure of the coronal magnetic field in an active region (AR).

Radio emission at decimeter wavelengths is associated with manifestations of numerous processes that determine the dissipation of magnetic field energy into the kinetic energy of accelerated particles at frequencies of 1–3 GHz. There are certain constraints for a detailed study of this process, since many phenomena radiate against the background of a powerful signal from the quiet Sun, which hinders high sensitivity and analysis of the fine frequency structure. At the same time, it is necessary to implement a large dynamic range to register the fine structure in the range from 10^{-3} s.f.u. to signals exceeding the level of a flux from the quiet Sun by tens of times during flare processes.

Despite available large interferometers operating in the radioheliograph mode, for a number of reasons, a large dynamic range can only be implemented on large instruments with a solid aperture of the collecting surface in a wide frequency range (Bogod, 2020).

Currently, such an instrument is the RATAN-600 reflector-type radio telescope, which already implements the mode of long-term tracking of the Sun using new technologies of radiometric signal reception. This instrument allows one to effectively use a large area of the receiving surface, cover a wide frequency range, conduct accurate polarization measurements, and perform multiazimuthal observations in a time interval of up to four hours.

New perspectives are opened by using a panoramic spectral radiometric complex (PSRC 1–3 GHz) with a high frequency resolution of 8192 channels/GHz (Bogod et al., 2023). A shortcoming is the moderate spatial resolution, which nevertheless allows distinguishing individual active structures on the solar disk. To eliminate the ambiguity in spatial resolution, we use high sensitivity to flux and polarization radiation for the comparison with AIA SDO maps for the studied structures.

An additional important factor is the spatial-frequency characteristic of the antenna that is continuous in all ranges, which, together with a high dynamic range (about 90 dB), contributes to the isolation of weak signals against the background of a powerful signal from the Sun.

Radio emission of the solar corona in the range of 1–3 GHz reflects processes associated with magnetic line reconnection in arch structures in the corona. These processes are fundamental for corona heating and occur in structures of various scales, down to nanoflares, according to the well-known model by Parker (1988). However, observational data in this range are strongly limited due to a large amount of industrial interferences (mobile communications, GPS, microwave ovens, aviation radars, etc.). On the other hand, some observational data (Bogod et al., 2001) indicate the presence of a fine structure (microbursts, spikes), for the study of which adequate radio astronomical equipment is required. In this work, we propose a new concept of spectroradiometry to use on the large RATAN-600 radio telescope, as well as consider its capabilities and the first results of its application for the analysis of radio emission from the solar corona. An important addition to the study of solar radio emission at RATAN-600 is putting into regular operation methods that expand the time range of observations (from 1 ms to 4 hours) by using the technology of multiazimuthal observations (Storozhenko et al., 2020). Applying high-speed registration methods (Ripak et al., 2023) contributes to obtaining new data on the frequency-time structure of solar quasiperiodic pulsations and to the registration of solar jets in active regions, etc. The effectiveness of observations will be enhanced by a new technique of high-speed registration with the removal of artificial interferences based on statistical methods (Lebedev et al., 2020).

2 Features of the new instrumentation

The PSRC was tested in the 1–3 GHz range. This range is currently heavily polluted by interference from mobile communications, aviation radars, and household microwave equipment. The use of high-speed technologies in the new spectral radiometry equipment allows effectively developing digital methods to eliminate interference.

The new experimental basis allows conducting observations with unprecedented frequency resolution in a wide frequency range and with a large dynamic range. In addition, it uses methods of multidimensional data processing (Drebushchak, 2013), which make it possible to implement multiobject observations and detect weak signals against the background of a strong signal.

2.1 On the achieved parameters of the new spectral complex

The new concept of spectral radiometry contains the following main principles:

1) rejection of the detection scheme as the main element of the radiometer and transition to direct digitization of the radio signal using high-speed analog-to-digital converters (ADCs);
2) creation of a system for high-speed spectrum registration in a wide frequency range;
3) conducting multichannel observations with the ultimate frequency resolution;
4) performing many hardware functions online (interference removal based on the assessment of spectral kurtosis), as well as other functions (calibration, stabilization, dynamic range correction, etc.);
5) application of multidimensional data processing methods.

The main parameters of the RATAN-600 reflector radio telescope are also included in the basis of the new concept, namely:

1) large instantaneous area of the radio telescope (500–1000 m^2);
2) wide operating multioctave frequency range (1–40 GHz);
3) smooth spatial-frequency characteristic throughout the entire frequency range of the radio telescope;
4) tracking mode of the selected object on the Sun for four hours in automatic mode.

As shown in Yesepkina et al. (1973), the quality of the radiometer frequency response is determined not only by the amplitude-frequency characteristic (AFC) of its amplifying path but also by the spatial-frequency characteristic of the antenna (SFC) and under the assumption of a clean (interference-free) environment in front of the radio telescope. Thus, the result is the Fourier product of two filters: SFC and AFC. This is especially important for broadband multioctave spectral radiometry systems. For reflector-type radio telescopes, the spatial-frequency characteristic $A_{uv}(f)$ is determined by the physical dimensions of the aperture and monotonously changes from the minimum value to the maximum operating frequency and is periodically calibrated.

2.2 Interference elimination

In the PSRC 1–3 GHz, interference is eliminated in three ways:

1. Filter (circuit) method for eliminating interference from mobile communications, aviation, TV, and household appliances.
2. Online method for assessing the gaussianity of spectral components according to statistical criteria, applied against medium-power interference. We use a method based on the assessment of kurtosis (the fourth moment of the distribution of signal power values), which allows distinguishing between signals of natural and artificial origin (Lebedev et al., 2022). Such preliminary cleaning allows for effective further data processing (Ovchinnikova et al., 2022).
3. Offline signal processing by the principal component method (Pomerantsev, 2008). High spectral resolution allows identifying processes in the selected spectral range or in individual regions of the Sun and determining their spectral structure. At this stage, the final signal cleaning from interference occurs (Ovchinnikova et al., 2022).

2.3 Sensitivity and dynamic range

For the large reflector instrument RATAN-600 in the solar observation mode, it is important to achieve a combination of high sensitivity and a large dynamic range. High sensitivity is used both for observations of reference radio sources (Fig. 1) and for spectral observations of weak coronal structures, for which a large effective area of the instrument is required. At the same time, a large dynamic range is important for detailed registration of both weak and powerful flare signals. To estimate the threshold sensitivity to the radio emission

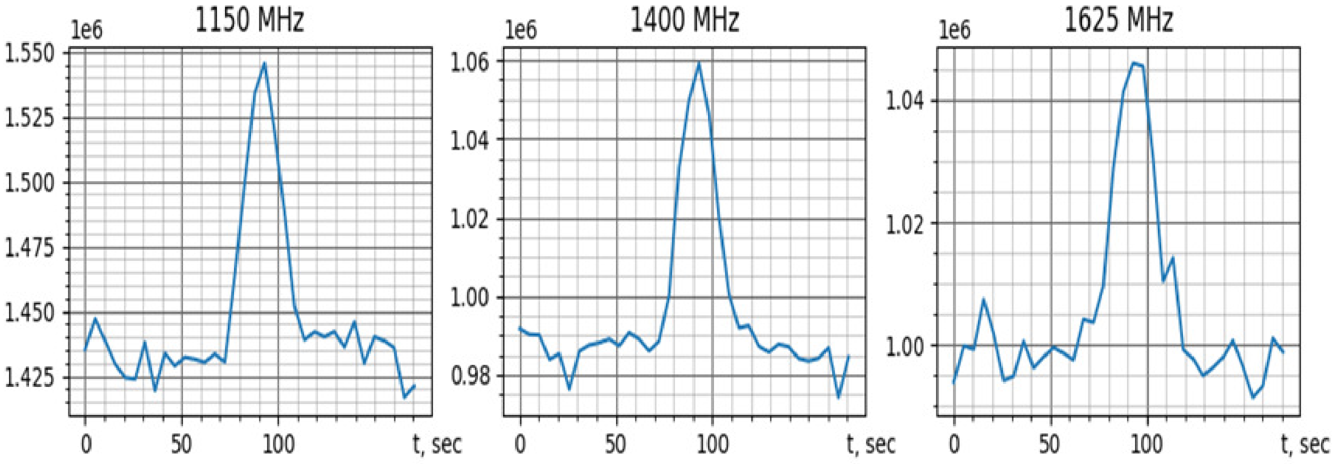

Fig. 1. Example of registration of a reference radio source: the Crab Nebula (NGC 1952) on June 28, 2021, Az = +12, sampling at several frequencies.

flux for a reflector telescope, the formula by Wilson (2013) is valid:

$$\Delta F_{\text{s.f.u.}} = \frac{2k(T_{\text{sys}} + \mu T_{\text{Sun}})}{A_{uv}(f) S \sqrt{(\Delta f n)\tau(n\Delta t)N}}. \quad (1)$$

Here:

- $\Delta F_{\text{s.f.u.}}$ is the radio telescope sensitivity to the radiation flux, s.f.u.;
- $k = 1.38 \cdot 10^{-23}$ W $\cdot$ m$^2 \cdot$ Hz^{-1} is the Boltzmann constant;
- $T_{\text{sys}} = T_{\text{a}} + T_{\text{rad}}$ are noise temperatures of the antenna and radiometer;
- μT_{Sun} is the temperature of the signal source, taking into account the antenna scattering coefficient;
- $A_{uv}(f)$ is the bandwidth of the spatial frequency filter u and v;
- S is the effective area of the RATAN-600 antenna (700–1000 m^2);
- $n \approx 10^4$ is the number of frequency channels;
- $\Delta f \approx 0.1$ MHz is the bandwidth of one channel;
- $(n\Delta t)N$ is the product of the time counts of readout $\tau = 10^{-3} \div 1$ s and the number of accumulation time intervals N in the tracking mode (from 8 ms to 600 s);
- $\Delta f / f = 10^{-4}$–10^{-5} is the relative frequency resolution;
- $\Delta t = 8$ ms/spectrum is the time resolution;
- $D = 90$ dB is the dynamic range.

2.4 Frequency resolution and wide frequency range

In the PSRC 1–3 GHz, a full coverage of the range is implemented, excluding the bands of rejection filters that suppress interference from mobile communications. The absolute frequency resolution $\Delta f = 120$ kHz has been achieved. This provides the number of frequency channels of 8192 and the relative frequency resolution $\Delta f / f = 10^{-4}$–10^{-5}. It is assumed to extend the concept to all frequency ranges of RATAN-600.

2.5 Temporal characteristics

The time resolution in the operating mode is $\Delta t = 8$ ms/spectrum. In the PSRC 1–3 GHz, time averaging is implemented within the range from 8 ms to 600 s. The azimuthal tracking mode in the Southern Sector with the Periscope is being refined (Ovchinnikova, Lebedev, 2023; Vakurin et al., 2023; Lebedev et al., 2023).

3 Processing of spectral data by the principal component analysis method

Large arrays of spectral data require new approaches to their processing. The maximum number of channels of the PSRC in the 1–3 GHz range is 8192 channels/GHz (i.e., 16384 intensity channels in each polarization). The duration of one solar observation is usually 150 s, which, with a resolution of 0.008 s, gives $150 \times 125 = 18750$ counts (Fig. 2). Thus, we have a data matrix of 16384×18750. To process and analyze multiwavelength RATAN-600 data, we used principal component analysis (Drebushchak, 2013). In the general data array, small-amplitude signals are difficult to distinguish against the background of a powerful signal from the Sun (Ovchinnikova et al., 2022). The representation of the original data array in the form of a matrix product eliminates the mutual correlation of variables and transforms the data space into the space of mutually orthogonal spectral components. These components are sorted according to their contribution to the total energy, and large-scale structures are represented by a small number of the first principal components. The remaining principal components give us the hidden variables that we are looking for, taking into account the signal-to-noise ratio. As applied to solar radio data, the following is sequentially identified:

1) a slowly varying radio component and the quiet Sun,
2) a rapidly varying component (bursts),
3) interfering components (interference),
4) noise components.

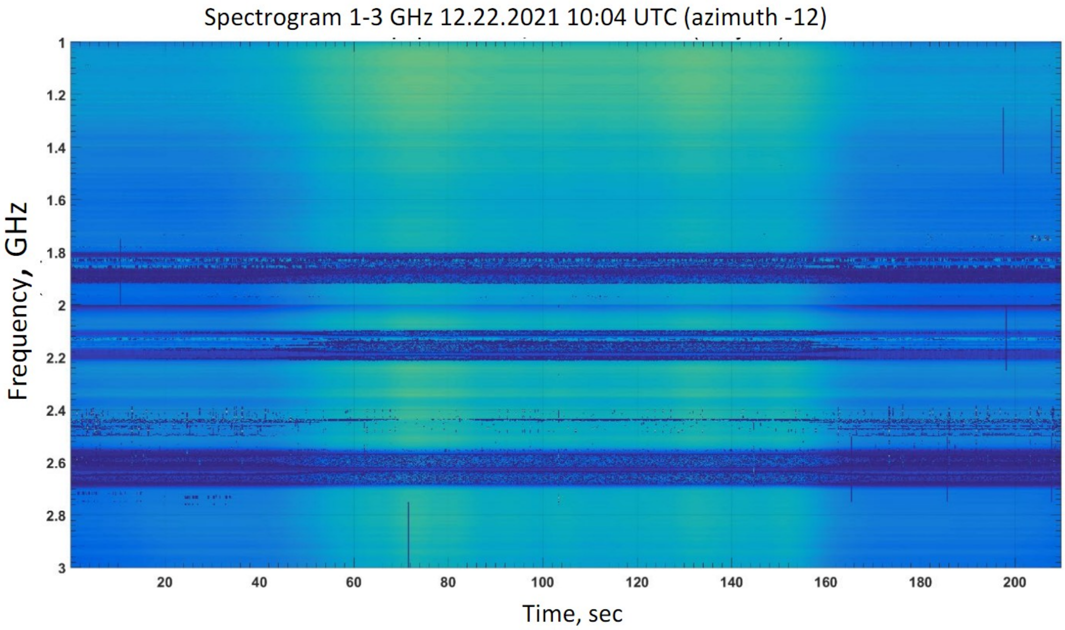

Fig. 2. Recording of a solar disk scan on December 22, 2021. The abscissa axis shows the recording time of 200 s with a resolution of 8 ms, and the ordinate axis shows the frequency range of 1–3 GHz with a resolution of 2 MHz. The spectrogram depicts three bands of rejection filters and dark pixels at the locations of interference, removed by the methods described in 2.2.

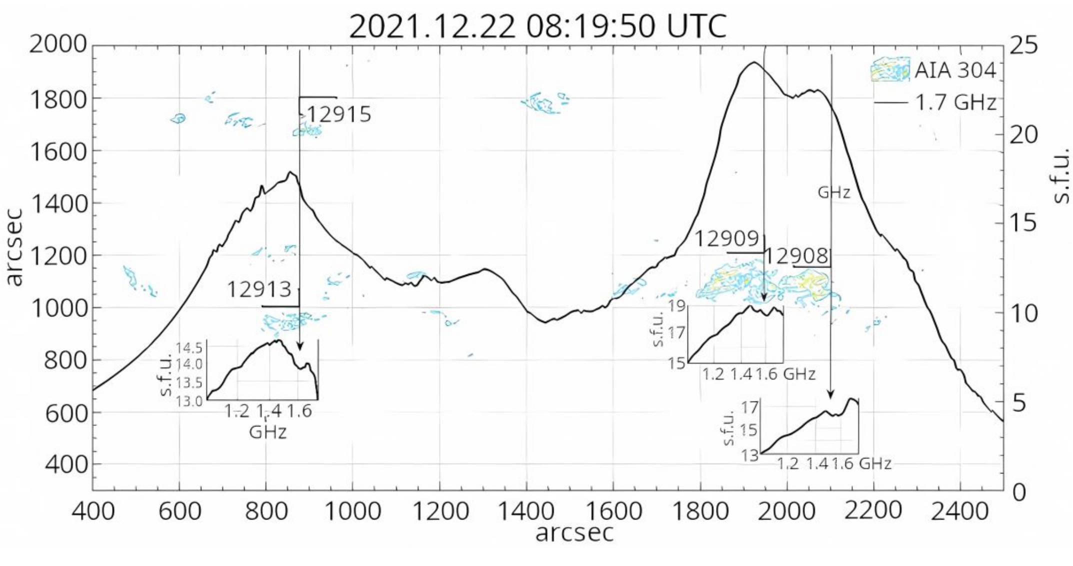

Fig. 3. Scan of the solar disk on December 22, 2021, at a frequency of 1.7 GHz with RATAN-600, superimposed on an SDO AIA image at a wavelength of 304 Å.

4 Observations of low-contrast formations with the PSRC 1–3 GHz

Registration of weak active formations on the Sun is an important observational task for all ranges, since it is of interest in light of the fundamental problem of solar corona heating. The main difficulty lies in the fact that the registration of such processes occurs against the background of a powerful signal from the quiet Sun, which makes it difficult to observe weak sources. In the radio range, a quantum of radiation has less energy than in the optical range and is able to carry information about weak significant processes. Since the sensitivity of the radio range is quite high, there is hope to elaborate methods for isolating weak signals against the background of strong ones.

Figure 3 shows one of the first observations of the Sun derived with the new spectral complex. The radio scan in a frequency channel of 1.7 GHz is superimposed on an SDO image (304 Å). The insets depict the emission spectra near AR 12907, 12909, and 12913. The spatial resolution

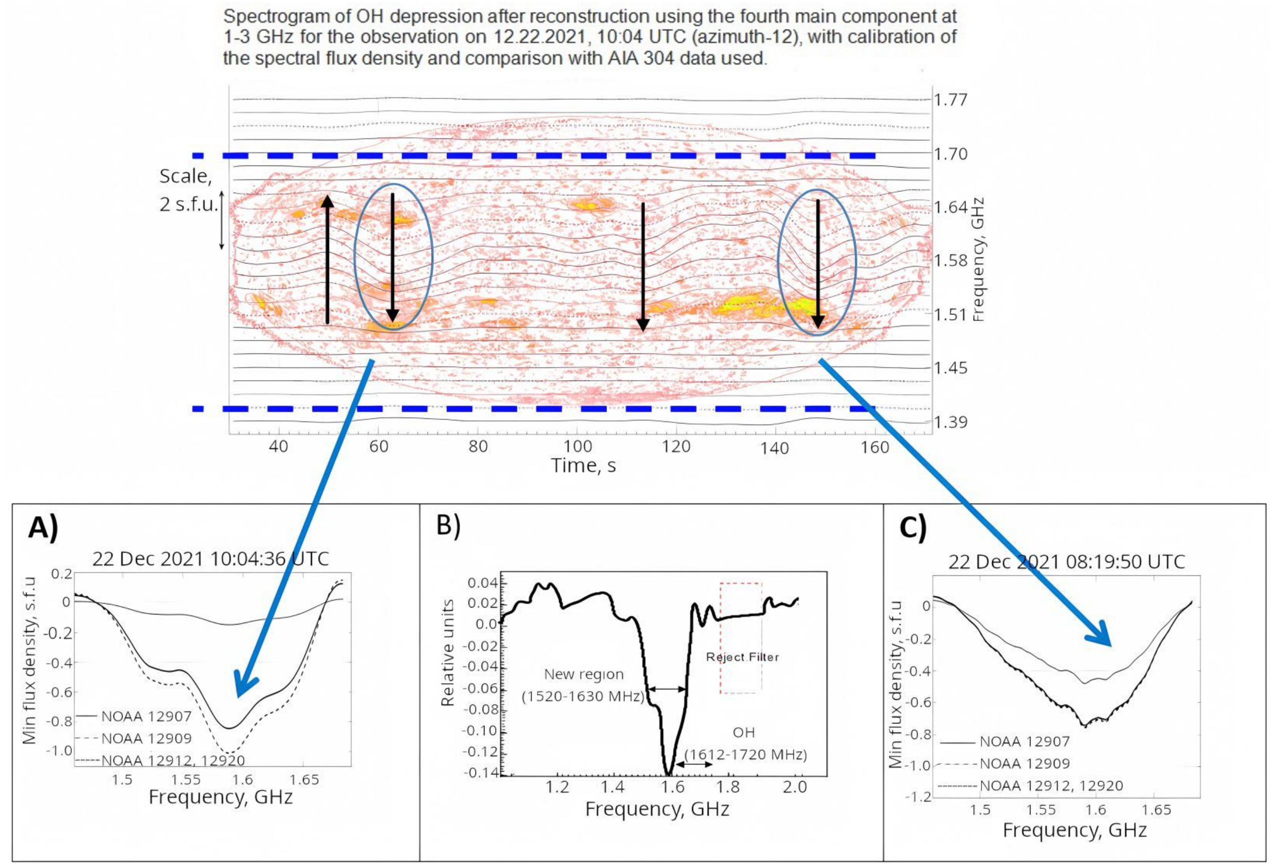

Fig. 4. Results of data processing for December 22, 2021.

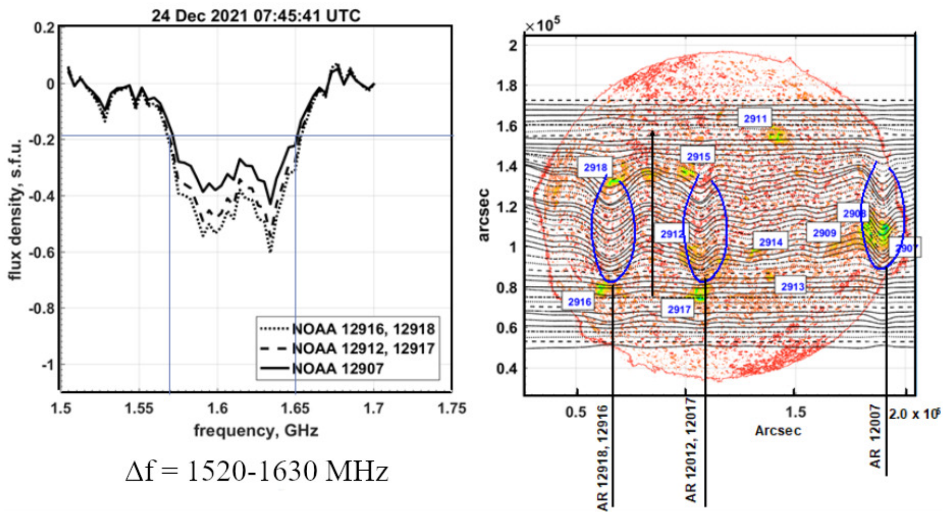

Fig. 5. Results of data processing for December 24, 2021.

of RATAN-600 in hour angle in this range is 2.5′. When processing all channels, one can notice weak spectral features (absorption bands, Ovchinnikova et al., 2023).

Figure 4 presents detailed data of this observation. As a result of processing using principal component decomposition, interference and powerful signals of the quiet Sun and active regions were removed. The upper figure shows the frequency channels with a resolution of 2 MHz/channel in the spectral section of 1.39–1.77 GHz, reconstructed without the spectral components of the background solar radiation and the powerful radiation of ARs. Arrows indicate sections of scans with absorption and brightening. The lower part of the figure shows the spectra of ARs in which absorption is observed. In the center one can see the spectral component of solar radiation, which indicates the presence of absorption in the range of 1520–1630 MHz. We note that the well-known in radio astronomy OH line (1612–1720 MHz) is located nearby.

Figure 5 shows the results of observations on December 24, 2021. Due to the rotation of the Sun, AR 12907 and 12912 took a new position, maintaining the absorption band in the spectrum, and regions 12916 and 12918 appeared in the east, in which absorption was also noted in the same frequency range (see the left part of the figure).

5 Analysis of observation results

Observations performed with a large dynamic range and high frequency resolution indicate the presence of a fine spectral structure in the solar corona above sunspots. Here, spectral inhomogeneity was discovered for the first time. Observations on December 22, 2021, recorded absorption regions (with a maximum of up to 0.6 s.f.u.) in NOAA AR 12907, 12909, and 12913 (see Figs. 3 and 4). On this day, there were also ARs on the disk in which absorption was absent. Thus, based on the results of the first series of observations, we can summarize the main observational facts.

1. In the range of 1520–1630 MHz, absorption bands are observed in individual regions of the Sun.
2. Absorption was observed only in the radiation of those ARs that were overlapped by a cold filament visible in Hα images and for limb ARs in the presence of a prominence – i.e., only where the existence of a hydroxyl group is potentially possible (Ovchinnikova et al., 2022; Ovchinnikova et al., 2023).
3. The regions in which absorption was noted were flare-active.
4. The magnitude of absorption is in the range of 0.2–0.6 s.f.u.
5. The absorption maximum is often projected onto the tail region of the sunspot group.

The main issue is the nature of the recorded absorption. Two preliminary versions are being considered. According to the first version, the dip in the spectrum may be associated with processes occurring in the active region. According to the second version, a group of lines is observed in the radio emission of ARs, presumably arising as a result of the splitting of the $X^2\Pi_{3/2}$ 0–0 and 1–1 levels in the ground state of the hydroxyl group, due to the anomalous Zeeman effect in the region of strong magnetic fields above ARs (Maeda et al., 2015). The results of recent observations (Ovchinnikova et al., 2022; Ovchinnikova et al., 2023), in particular in the tracking mode with high frequency resolution, confirm the latter version.

Further study of these phenomena will indicate their physical nature.

6 Conclusions

The work is devoted to the first results of observations made with a new high-frequency spectral complex in the frequency range of 1–3 GHz at the RATAN-600 radio telescope. The achieved high sensitivity is confirmed by methods for registering weak signals both in brightening and absorption at a level of about 10^{-3}–10^{-4} s.f.u. on the solar disk. This indicates the temperature inhomogeneity of the corona in the studied frequency range. Several new effects were noticed: absorption in the range of 1520–1630 MHz and uneven thermal distribution in detailed temperature spectra. A preliminary interpretation is proposed, which needs to be further elaborated.

Acknowledgments. Observations at the SAO RAS telescopes are supported by the Ministry of Science and Higher Education of the Russian Federation. The instrumentation upgrade is implemented within the framework of the national project "Science and Universities".

The work was carried out within the state assignment of the SAO RAS, approved by the Ministry of Science and Higher Education of the Russian Federation.

References

Bogod V.M., 2020. In I.I. Romanyuk, I.A. Yakunin, A.F. Valeev, D.O. Kudryavtsev (Eds.), Ground-Based Astronomy in Russia. 21st Century. pp. 399–404. doi:10.26119/978-5-6045062-0-2_2020_399.

Bogod V.M., Mercier C., Yasnov L.V., 2001. J. Geophys. Res., vol. 106, no. A11, pp. 25353–25360.

Bogod V.M., Lebedev M.K., Ovchinnikova N.E., Ripak A.M., Storozhenko A.A., 2023. Cosmic Research, vol. 61, no. 1, pp. 27–33.

Drebushchak T.N., 2013. Introduction to chemometrics: Textbook. Novosibirsk: Novosibirsk State University.

Lebedev M., Ripak A., Bogod V., 2020. In I.I. Romanyuk, I.A. Yakunin, A.F. Valeev, D.O. Kudryavtsev (Eds.), Ground-Based Astronomy in Russia. 21st Century. pp. 413–416. doi:10.26119/978-5-6045062-0-2_2020_413.

Lebedev M.K., Ovchinnikova N.E., Bogod V.M., Ripak A.M., Storozhenko A.A., 2022. Proc. Science, vol. MUTO2022, p. 006.

Lebedev M.K., Ovchinnikova N.E., Storozhenko A.A., 2023. In Modern Instruments and Methods in Astronomy, All-Russian Conference Proceedings. p. 8.

Maeda K., Wall M.L., Carr L.D., 2015. New Journal of Physics, vol. 17, no. 4, p. 045014.

Ovchinnikova N.E., Lebedev M.K., Bogod V.M., Ripak A.M., Storozhenko A.A., 2022. Proc. Science, vol. MUTO2022, p. 007.

Ovchinnikova N.E., Bogod V.M., Lebedev M.K., 2023. Proceedings of the XXVII All-Russian Annual Conference on Solar Physics "Solar and Solar-Terrestrial Physics – 2023", p. 245.

Ovchinnikova N.E., Lebedev M.K., 2023. Modern Instruments and Methods in Astronomy, All-Russian Conference Proceedings, p. 8.

Parker E.N., 1988. Astrophys. J., vol. 330, p. 474.

Pomerantsev A., 2008. Principal component analysis (PCA). Available at: https://rcs.chemometrics.ru/ru/books/metod-glavnykh-komponent/.

Ripak A.M., Bogod V.M., Grenkov S.A., Lebedev M.K., 2023. Astrophys. Bull., vol. 78, no. 4, p. 465.

Storozhenko A., Lebedev M., Ovchinnikova N., et al., 2020. In I.I. Romanyuk, I.A. Yakunin, A.F. Valeev, D.O. Kudryavtsev (Eds.), Ground-Based Astronomy in Russia. 21st Century. pp. 407–408. doi:10.26119/978-5-6045062-0-2_2020_407.

Vakurin V.S., Storozhenko A.A., Zharov V.I., Grechkin A.A., 2023. In Modern Instruments and Methods in Astronomy, All-Russian Conference Proceedings. p. 5.

Wilson T.L., 2013. In T.D. Oswalt, H.E. Bond (Eds.), Planets, Stars and Stellar Systems. Volume 2: Astronomical Techniques, Software and Data. p. 283. doi:10.1007/978-94-007-5618-2_6.

Yesepkina N.A., Korol'kov D.V., Pariiskii Y.N., 1973. Radio telescopes and radiometers. M.: Nauka.